Exploring hadronic de-excitation via Lepton Flavor Violation

Fabiola Fortuna,[*] Leonardo Esparza,[†] and Genaro Toledo[‡]

Instituto de Física, Universidad Nacional Autónoma de México, AP 20-364, México D.F. 01000, México

(Dated: May 6, 2024)

In this work, we consider a particular case of hadronic de-excitation via lepton flavor violation (LFV). Namely, $\rho' \to \rho\mu e$ decay, described considering effective dim-5 and dim-7 operators. Using the current bounds for the couplings from direct processes, we exhibit the different features in the dilepton invariant mass distribution and the branching ratios, depending on the effective operator. The results, although heavily suppressed, show that they may be useful to impose constraints on individual contributions and help to disentangle them, when complemented with observables from nuclei. Our particular case can be taken as an initial step to look for other hadronic states, such as in quarkonia, where the de-excitation can have enough energy to search for LFV involving the τ lepton.

I. INTRODUCTION

Meson decays have been explored in the search of LFV considering transitions of the form $q \to q' l_i^+ l_j^-$, which involves a quark transition simultaneously [1–4]. There, the use of effective operators including both leptons and quarks, provides useful information to place bounds on the branching ratios of such decays, which necessarily involve different quark structure of the initial and final mesons. These transitions have been studied for heavy to light mesons within the effective field theory (EFT) framework, for instance in Ref. [4], where LHC data was used to derive upper limits on LFV $B_{(s)}$ and D meson decays. LFV in meson decays has also been investigated within particular model realizations, for instance, in Ref. [5] these processes were studied in the U(1)$_X$SSM. On the other hand, scenarios involving direct processes such as $\mu \to e\gamma$ are free of the hadronic part and offer clean bounds which are expected to be further improved in the near future.

Another scenario which has received less attention is at the interplay of those mentioned above. Namely, the one involving hadronic states with the same initial and final quarks. This feature has been used to place bounds on the LFV in nuclei, using an EFT approach to describe such processes [6]. This has proven to be a possible way to deepen the understanding in nuclear matters in experiments such as NA64 [7] where the limitations are set by the nuclear effects to be properly accounted at the given precision. This kind of process allows to explore dim-5 and dim-7 operators involving one and two photons intermediate states, which then produce the LFV pair. The dim-5 and dim-7 effective operators have been used previously to explore LFV decays and LFV in nuclei [6, 8–11].

A possible hadronic scenario for the same effective approach is the use of radially excited hadronic states, whose de-excitation process goes via a LFV mechanism. One example is the ρ' meson which is de-excited decaying into a ρ meson and the LFV pair, as depicted in Figs. 3 and 4. This scenario is a cleaner channel to search for LFV than the conversion processes in nuclei as it is free from nuclear effects, although a proper knowledge of the hadronic form factors of the transition is required.

In this work, we consider this particular process to illustrate the main features of the hadronic de-excitation involving LFV effects and the role of the effective operators involved. Namely, the $\rho' \to \rho\mu e$ decay, and determine at which extent they can offer new features of LFV in low energy hadronic states. We use the EFT approach to describe the LFV vertices [10], while the hadronic side is described using the vector meson dominance model (VMD) [12–14]. In section II, we introduce the dim-5 and dim-7 effective operators that describe the charged LFV processes, and the constraints that we derive on the effective coefficients from a direct experimental search. In section III, we outline the $\rho' \to \rho\mu e$ decay amplitude incorporating the VMD hadronic interaction. This decay process is generated at tree level with the dim-5 operators and at one-loop level with the dim-7 operators. Section IV is devoted to present our results on the dilepton invariant mass and branching ratio, and the discussion of the different features associated to each operator.

II. EFFECTIVE FIELD THEORY DESCRIPTION

In this work we use effective operators that generate charged lepton flavor violating interactions. Particularly, we focus on the $\mu e\gamma$ and $\mu e\gamma\gamma$ effective interactions. The former is generated by the dim-5 dipole operator shown in Eq. (1) while the latter is produced by the dim-7 diphoton operator in Eq. (2) [15].

$$\mathcal{L}_{\text{dim-5}} = D_R^{\mu e} \bar{\mu}_L \sigma_{\mu\nu} e_R F^{\mu\nu} + D_L^{\mu e} \bar{\mu}_R \sigma_{\mu\nu} e_L F^{\mu\nu} + h.c.,$$

(1)

---

[*] fabyfortuna@fisica.unam.mx
[†] leonardoesparza@estudiantes.fisica.unam.mx
[‡] toledo@fisica.unam.mx

where the subscripts $L(R)$ indicate the chirality of the lepton.

$$\mathcal{L}_{\text{dim-7}} = (G_{SR}^{\mu e}\bar{\mu}_L e_R + G_{SL}^{\mu e}\bar{\mu}_R e_L)\, F_{\mu\nu}F^{\mu\nu}$$
$$+ \left(\tilde{G}_{SR}^{\mu e}\bar{\mu}_L e_R + \tilde{G}_{SL}^{\mu e}\bar{\mu}_R e_L\right)\tilde{F}_{\mu\nu}F^{\mu\nu} + \text{h.c.}, \quad (2)$$

with $\tilde{F}_{\mu\nu} = \frac{1}{2}\epsilon_{\mu\nu\sigma\lambda}F^{\sigma\lambda}$ the dual electromagnetic field-strength tensor.

Recently, in Ref. [10] these operators were used to derive indirect upper limits in the $\ell_i \to \ell_j\gamma\gamma$ decays from the experimental limits on the $\ell_i \to \ell_j\gamma$ processes. Taking the decay rates computed there, shown in Eq. (3), and comparing them with the current experimental upper limit on the $\mu \to e\gamma$ decay [16] we obtained updated constraints in the $D^{\mu e}$ and $G^{\mu e}$ effective coefficients, that will be used in the computation of the observables. These constraints are shown in Table I.

$$\Gamma(\mu \to e\gamma)\big|_{\text{dim-5}} = \frac{m_\mu^3}{4\pi}\big|D^{\mu e}\big|^2,$$

$$\Gamma(\mu \to e\gamma)\big|_{\text{dim-7}} \sim \frac{\alpha|G_{\mu e}|^2}{256\pi^4}m_\mu^7\log^2\left(\frac{\Lambda^2}{m_\mu^2}\right), \quad (3)$$

where $\big|D^{\mu e}\big|^2 = \big|D_R^{\mu e}\big|^2 + \big|D_L^{\mu e}\big|^2$ and $\big|G_{\mu e}\big|^2 = \big|G_{SR}^{\mu e}\big|^2 + \big|G_{SL}^{\mu e}\big|^2 + \big|\tilde{G}_{SR}^{\mu e}\big|^2 + \big|\tilde{G}_{SL}^{\mu e}\big|^2$. In the decay rate computed with the dim-7 operators, we are taking only the leading term, and we use $\Lambda = 100$ GeV to derive the constraint on $G_{\mu e}$ shown in Table I.

Coefficient	Constraint
$\big|D^{\mu e}\big|$	3.1×10^{-14} GeV^{-1}
$\big|G_{\mu e}\big|$	1.1×10^{-10} GeV^{-3}

TABLE I. Constraints on the effective coefficients $D^{\mu e}$ and $G_{\mu e}$ from the current experimental upper limit on $\mu \to e\gamma$ decay (BR$(\mu \to e\gamma) < 3.1 \times 10^{-13}$ at 90%CL) [16].

Due to the expected sensitivity for $\mu \to e$ conversion process, of order 10^{-16}, according to upcoming experiments [17], we expect that in the future the best probe for $\mu e\gamma$ and $\mu e\gamma\gamma$ operators will come from these $\mu \to e$ conversion process. New-physics scenarios where the inelastic $\mu \to e$ conversion can provide additional information on LFV are explored in [18].

III. THE $\rho' \to \rho\mu e$ DECAY

The $\rho(1450)$, generally denoted as the ρ' meson, is a radially excited vector state, observed in low energy experiments [19–24]. It has been noticed that it plays an important role in the description of low energy observables described in the VMD approach [25]. The expected continuation of the efforts to increase the luminosity of such experiments will include a large ρ' production, opening the possibility to explore non-conventional processes, as the one we present here.

In the following we describe the $\rho' \to \rho\mu e$ decay, we compute its amplitude considering dim-5 and dim-7 effective operators.

A. Dim-5 operator driven process

We first calculate the $\rho'^{\pm}(q, \eta) \to \rho^{\pm}(p, \epsilon^*)\mu^-(l_1)e^+(l_2)$ decay, where η and ϵ^* correspond to the polarization vectors of the ρ' and ρ mesons, respectively, when the dominant contribution is driven by the dim-5 operators in Eq. (1). This allows to describe the process at tree level, as shown in Fig. 3. The amplitude for this diagram can be written as:

$$\mathcal{M}_{\text{dim5}} = -\frac{e\, g_{\rho'\rho\gamma}}{k^2}\ell_{\mu\nu}(k^\mu g^{\nu\gamma} - k^\nu g^{\mu\lambda})\Gamma_{\alpha\beta\gamma}(q, k)\eta^\alpha\epsilon^{*\beta}, \quad (4)$$

where $k = q-p$ is the transferred momentum into the lepton pair, described by $\ell_{\mu\nu} = \bar{u}_1\sigma_{\mu\nu}(D_R^{\mu e}P_R + D_L^{\mu e}P_L)v_2$, according to the effective operator in Eq. (1). On the hadronic side, the $\rho' \to \rho\gamma$ transition is modeled following the general structure expected for a $V'V\gamma$ vertex, with two distinct vectors (V and V') and a photon [26, 27]. Thus the corresponding vertex, $\Gamma_{\alpha\beta\gamma}(q, k)$, can be parameterized in terms of the magnetic dipole moment and electric quadrupole transition operators, as follows:

$$\Gamma_{\alpha\beta\gamma}(q, k) = \beta(g^{\alpha\beta}k^\alpha - g^{\gamma\alpha}k^\beta)$$
$$+ \frac{\gamma}{2m_{\rho'}^2}\left[(2q-k)^\gamma k^\alpha k^\beta - q\cdot k(g^{\beta\gamma}k^\alpha + g^{\gamma\alpha}k^\beta)\right]. \quad (5)$$

Notice that each contribution is gauge invariant by itself. The corresponding strengths β and γ, for the dipole and quadrupole interactions, respectively, are free parameters. We are not aware of a quark model estimate of such couplings for this particular case [1]. However in transitions of the form $VV\gamma$ they are around $\beta = 2$ and $\gamma = 1$ [30]. Thus, we consider these values as a reference of their magnitudes.

The global strength, is set by $e\, g_{\rho'\rho\gamma}$, where the $g_{\rho'\rho\gamma}$ coupling is taken as the ratio of the g_ρ and $g_{\rho'}$ couplings, in analogy to VMD idea, where g_V accounts for the vector interaction with the photon. We use both possibilities $g_\rho/g_{\rho'} = 0.38$ and $g_{\rho'}/g_\rho = 2.60$ [25].

B. Dim-7 operator driven process

We now consider scenarios where the dim-5 operators are suppressed, while the dim-7 operators are not (as

---

[1] The radiative decay of radial excitations considered in quark models are typically of the form $V \to P\gamma$ [28, 29].

discussed in Sec. IV of Ref. [10]).

The $\rho' \to \rho\mu e$ decay is a one-loop level process when driven by the dim-7 operators shown in Eq. (2), and the corresponding Feynman diagram is depicted in Fig. 4. The loop involves a pion and a generic vector-pseudoscalar-photon interaction, which is described by the effective Lagrangian

$$\mathcal{L} = g_{VP\gamma}\epsilon_{\alpha\beta\mu\nu}\partial^\alpha V^\beta \partial^\mu A^\nu P, \tag{6}$$

where V, A and P are the vector, photon and pseudo-scalar fields, respectively. The $g_{VP\gamma}$ couplings can be obtained using VMD relations between radiative and hadronic couplings, $g_{\rho'\pi\gamma} = g_{\rho'\omega\pi}e/g_\omega = 0.063$ and $g_{\rho\pi\gamma} = g_{\rho\omega\pi}e/g_\omega = 0.206$. These values were obtained from a previous analysis of low energy couplings in the same approach [25].

The amplitude corresponding to the diagram in Fig. 4 is twofold, depending on which structure is used to describe the two photons coupled to the LFV pair. That is, proportional to the EM tensor (here labeled by F) or to the dual EM tensor ($\tilde{F}$) as shown below:

$$\mathcal{M}_{\mathrm{dim7}(F)} = 2\ell^F \Gamma^F_{\alpha\beta}\eta^\alpha \epsilon^{*\beta}, \tag{7}$$

$$\mathcal{M}_{\mathrm{dim7}(\tilde{F})} = 2\ell^{\tilde{F}} \Gamma^{\tilde{F}}_{\alpha\beta}\eta^\alpha \epsilon^{*\beta}, \tag{8}$$

where $\ell^{\overset{(\sim)}{F}} = \bar{u}_1(\overset{(\sim)}{G}{}^{\mu e}_{SR}P_R + \overset{(\sim)}{G}{}^{\mu e}_{SL}P_L)v_2$, according to Eq. (2) and the structures resulting from the evaluation of the loop are $\Gamma^F_{\alpha\beta}$ and $\Gamma^{\tilde{F}}_{\alpha\beta}$, given by

$$\Gamma^F_{\alpha\beta} = \frac{ig_{\rho'\pi\gamma}\,g_{\rho\pi\gamma}}{16\pi^2}\left\{ f_1(m^2_{12})p_\alpha q_\beta + f_2(m^2_{12})g_{\alpha\beta}) \right\},$$

$$\Gamma^{\tilde{F}}_{\alpha\beta} = \frac{ig_{\rho'\pi\gamma}\,g_{\rho\pi\gamma}}{16\pi^2}\epsilon_{\alpha\beta\mu\nu}p^\mu q^\nu f_3(m^2_{12}), \tag{9}$$

where f_1, f_2 and f_3 are loop functions that depend on the lepton invariant mass, $m^2_{12} = (l_1 + l_2)^2$. In Fig. 5, we show the behavior of the magnitude of these functions. We use Package-X [31] for the analytical evaluation of the loop integrals. For the numerical evaluation, we use the COLLIER library [32], considering only the finite part and a cut-off of $\mu = 1$ GeV, expected to be valid for hadronic functions. Energy dependent couplings (form factors) in the vertices would soften the divergent part, but small effects are expected given the relatively low energy transfer.

IV. RESULTS AND DISCUSSION

Using the standard kinematics as given in PDG [33] we compute the dilepton invariant mass distribution and the branching ratios (BR) for the different amplitudes presented above.

In Figs. 1 and 2, we show the dilepton invariant mass distributions of the differential decay rate $d\Gamma/dm_{12}$
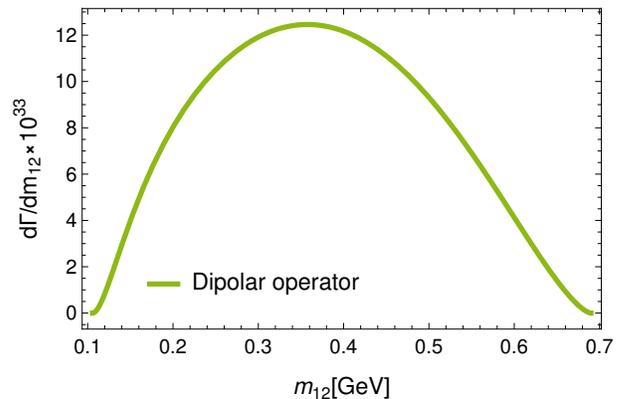

FIG. 1. Dilepton invariant mass distribution for the $\rho' \to \rho\mu e$ decay driven by the dim-5 operators, taking $g_{\rho'\rho\gamma} = 1$ (cf. Eq. (4)).
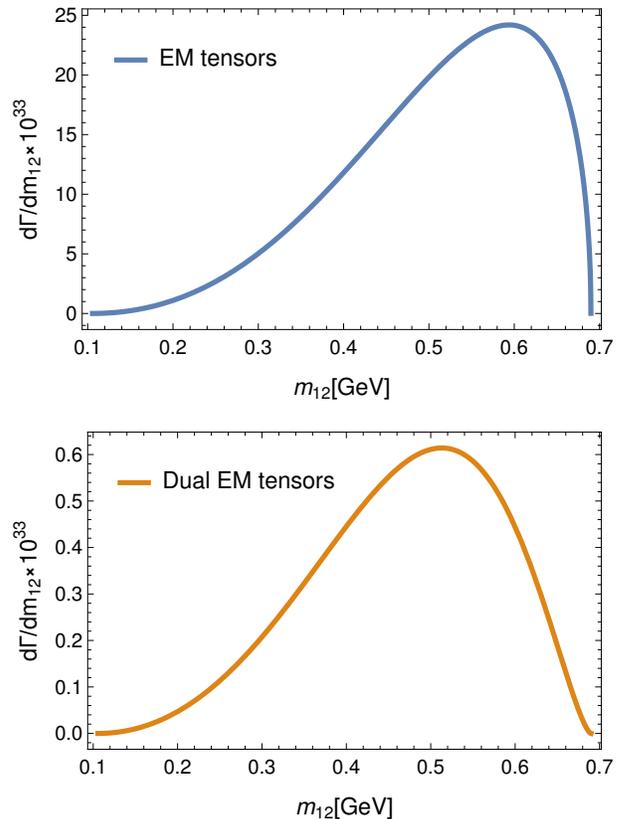

FIG. 2. Dilepton invariant mass distribution for the $\rho' \to \rho\mu e$ decay driven by the dim-7 operators. The upper panel corresponds to the EM tensor (Eq. (7)) and the lower panel corresponds to the dual EM tensor (Eq. (8)).

driven by the dim-5 and dim-7 operators, respectively. For the latter, the upper panel corresponds to the EM tensor (Eq. (7)) and the lower panel corresponds to the dual EM tensor (Eq. (8)). This observable allows to distinguish the different energy behavior among them, the dim-5 operators generate a curve slightly tilted towards

Operator	BR($\rho' \to \rho\mu e$)
Dim-5 dipolar	$[1.7 - 77.8] \times 10^{-33}$
Dim-7 EM	1.7×10^{-32}
Dim-7 Dual EM	4.4×10^{-34}

TABLE II. $\rho' \to \rho\mu e$ branching ratios driven by the dim-5 and dim-7 operators. The interval obtained by using the dipolar operator corresponds to the values we used for the $g_{\rho'\rho\gamma}$ coupling.

the left, while the dim-7 operators produce curves tilted to the right. The relative magnitude among the dim-7 operators comes from the evaluation of the loop. At the amplitude level, the EM tensor part is an order of magnitude larger than the dual EM tensor. This can be seen from the magnitude of the loop functions in Fig. 5. Besides the relative magnitude, the $d\Gamma/dm_{12}$ from the EM tensor (upper panel in Fig. 2) generates a curve whose peak is more shifted towards the end of the plot with respect to the dual EM one (lower panel in Fig. 2). Note that in the one-loop level process, the lepton pair is emitted in s-wave.

The branching ratios obtained using the dim-5 and dim-7 operators are shown in Table II. For the dim-5 operators, we quote an interval for the branching ratio obtained from the different values used for the $g_{\rho'\rho\gamma}$ coupling. That is, they produce a difference of around two orders of magnitude. We also explored the structure of the $\rho'\rho\gamma$ vertex, Eq. (5), and found that the dominant contribution comes from the dipolar magnetic interaction, while the quadrupolar electric interaction has a relative suppression of about two orders of magnitude.

The difference in magnitude for the BR of the two dim-7 contributions follows the same argument as in the dilepton invariant mass distribution. It is interesting to note that the relative magnitude is opposite to the one obtained from interactions in nuclei [6] where the dominant contribution is driven by the dual EM tensors while in our case it is the EM (see table II). This feature offers the possibility to disentangle both contributions from complementary observables. However, notice that this is not a general statement, since the observation is drawn from two different systems. While we are working with an effective vertex involving an electron and a muon, in Ref. [6] they analyzed the light lepton to tau conversion.

We have considered the vector mesons as stable states. Further considerations to describe the full process of production and decay would require to incorporate their finite decay width, which is out of the scope of this work. In the experimental side, considerations regarding the reconstruction of the vector states is already part of the data analysis procedures as exemplified in the detection of such states.

In this work, we have explored a particular case of

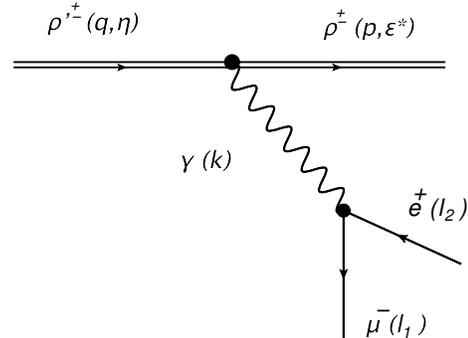hadronic de-excitation via LFV, and the different fea-

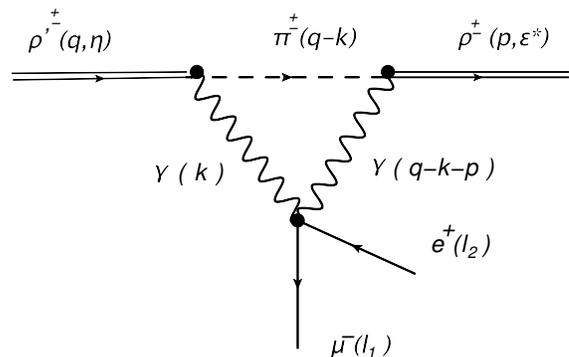FIG. 3. $\rho' \to \rho\mu e$ decay driven by the dim-5 effective operator.

FIG. 4. $\rho' \to \rho\mu e$ decay driven by the dim-7 effective operator.

tures they can exhibit, depending on the effective operator producing the LFV pair. The results, although heavily suppressed, show that they may be useful to impose constraints on individual contributions and help to disentangle them, when complemented with observables from nuclei. This work, as others in the low energy regime exploring hyperon decays via majorana neutrinos ([34]) are interesting on their own. Low energy experiments are reaching a high luminosity stage where this kind of hadrons are copiously produced, which opens the possibility to explore this type of scenarios not yet considered. Our particular case can be taken as an initial step to look for other hadronic states, such as in quarkonia, where the de-excitation can have higher energy to search for LFV involving the τ lepton.
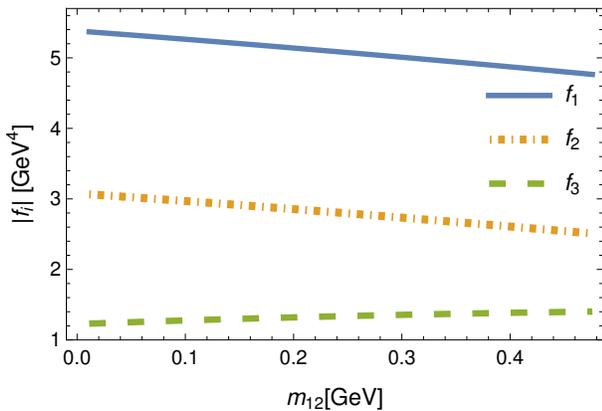
FIG. 5. Magnitude of the f_1, f_2 and f_3 loop functions. $|f_1|$ and $|f_3|$ are multiplied by $p \cdot q$ to be dimensionally consistent with each other.

[1] S. L. Glashow, D. Guadagnoli, and K. Lane, Lepton Flavor Violation in B Decays?, Phys. Rev. Lett. **114**, 091801 (2015), arXiv:1411.0565 [hep-ph].

[2] L. Calibbi and G. Signorelli, Charged Lepton Flavour Violation: An Experimental and Theoretical Introduction, Riv. Nuovo Cim. **41**, 71 (2018), arXiv:1709.00294 [hep-ph].

[3] D. Bečirević, O. Sumensari, and R. Zukanovich Funchal, Lepton flavor violation in exclusive $b \to s$ decays, Eur. Phys. J. C **76**, 134 (2016), arXiv:1602.00881 [hep-ph].

[4] S. Descotes-Genon, D. A. Faroughy, I. Plakias, and O. Sumensari, Probing lepton flavor violation in meson decays with LHC data, Eur. Phys. J. C **83**, 753 (2023), arXiv:2303.07521 [hep-ph].

[5] X.-X. Dong, S.-M. Zhao, J.-P. Huo, T.-T. Wang, Y.-T. Wang, and T.-F. Feng, Search for charged lepton flavor violation of vector mesons in the U(1)$_X$SSM, (2024), arXiv:2402.11240 [hep-ph].

[6] F. Fortuna, X. Marcano, M. Marín, and P. Roig, Lepton flavor violation from diphoton effective interactions, Phys. Rev. D **108**, 015008 (2023), arXiv:2305.04974 [hep-ph].

[7] S. Gninenko, S. Kovalenko, S. Kuleshov, V. E. Lyubovitskij, and A. S. Zhevlakov, Deep inelastic $e - \tau$ and $\mu - \tau$ conversion in the NA64 experiment at the CERN SPS, Phys. Rev. D **98**, 015007 (2018), arXiv:1804.05550 [hep-ph].

[8] S. Davidson, Y. Kuno, and M. Yamanaka, Selecting $\mu \to e$ conversion targets to distinguish lepton flavour-changing operators, Phys. Lett. B **790**, 380 (2019), arXiv:1810.01884 [hep-ph].

[9] S. Davidson, Y. Kuno, Y. Uesaka, and M. Yamanaka, Probing $\mu e\gamma\gamma$ contact interactions with $\mu \to e$ conversion, Phys. Rev. D **102**, 115043 (2020), arXiv:2007.09612 [hep-ph].

[10] F. Fortuna, A. Ibarra, X. Marcano, M. Marín, and P. Roig, Indirect upper limits on $\ell_i \to \ell_j \gamma\gamma$ from $\ell_i \to \ell_j \gamma$, Phys. Rev. D **107**, 015027 (2023), arXiv:2210.05703 [hep-ph].

[11] V. Cirigliano, K. Fuyuto, M. J. Ramsey-Musolf, and E. Rule, Next-to-leading order scalar contributions to $\mu \to$e conversion, Phys. Rev. C **105**, 055504 (2022), arXiv:2203.09547 [hep-ph].

[12] M. Bando, T. Kugo, S. Uehara, K. Yamawaki, and T. Yanagida, Is rho Meson a Dynamical Gauge Boson of Hidden Local Symmetry?, Phys. Rev. Lett. **54**, 1215 (1985).

[13] T. Fujiwara, T. Kugo, H. Terao, S. Uehara, and K. Yamawaki, Nonabelian Anomaly and Vector Mesons as Dynamical Gauge Bosons of Hidden Local Symmetries, Prog. Theor. Phys. **73**, 926 (1985).

[14] U. G. Meissner, Low-Energy Hadron Physics from Effective Chiral Lagrangians with Vector Mesons, Phys. Rept. **161**, 213 (1988).

[15] J. Bowman, T. Cheng, L.-F. Li, and H. Matis, New Upper Limit for $\mu \to e\gamma\gamma$, Phys. Rev. Lett. **41**, 442 (1978).

[16] K. Afanaciev et al. (MEG II), A search for $\mu^+ \to$ e$^+\gamma$ with the first dataset of the MEG II experiment, Eur. Phys. J. C **84**, 216 (2024), arXiv:2310.12614 [hep-ex].

[17] F. Abdi et al. (Mu2e), Mu2e Run I Sensitivity Projections for the Neutrinoless $\mu^- \to e^-$ Conversion Search in Aluminum, Universe **9**, 54 (2023), arXiv:2210.11380 [hep-ex].

[18] W. C. Haxton and E. Rule, Distinguishing charged lepton flavor violation scenarios with inelastic $\mu \to e$ conversion, (2024), arXiv:2404.17166 [hep-ph].

[19] B. Diekmann, Spectroscopy of Mesons Containing Light Quarks (u, d, s) or Gluons, Phys. Rept. **159**, 99 (1988).

[20] L. M. Kurdadze, M. Y. Lelchuk, E. V. Pakhtusova, V. A. Sidorov, A. N. Skrinsky, A. G. Chilingarov, Y. M. Shatunov, B. A. Shvarts, and S. I. Eidelman, MEASURING OF PION FORM-FACTOR WITHIN THE REGION S**(1/2) FROM 640-MEV TO 1400-MEV, JETP Lett. **37**, 733 (1983).

[21] M. N. Achasov et al., Updated measurement of the $e^+e^- \to \omega\pi^0 \to \pi^0\pi^0\gamma$ cross section with the SND detector, Phys. Rev. D **94**, 112001 (2016), arXiv:1610.00235 [hep-ex].

[22] J. P. Lees et al. (BABAR, BaBar), Study of the process $e^+e^- \to \pi^+\pi^-\pi^0$ using initial state radia-

tion with BABAR, Phys. Rev. D **104**, 112003 (2021), arXiv:2110.00520 [hep-ex].

[23] M. Ablikim *et al.* (BESIII), Measurement of the $e^+e^- \rightarrow \pi^+\pi^-\pi^0$ Cross Section from 0.7 GeV to 3.0 GeV via Initial-State Radiation, (2019), arXiv:1912.11208 [hep-ex].

[24] M. Fujikawa *et al.* (Belle), High-Statistics Study of the tau- —> pi- pi0 nu(tau) Decay, Phys. Rev. D **78**, 072006 (2008), arXiv:0805.3773 [hep-ex].

[25] G. Ávalos, A. Rojas, M. Sánchez, and G. Toledo, Role of the $\rho(1450)$ in low-energy observables from an analysis in the meson dominance approach, Phys. Rev. D **107**, 056006 (2023), arXiv:2211.14380 [hep-ph].

[26] J. F. Nieves and P. B. Pal, Electromagnetic properties of neutral and charged spin 1 particles, Phys. Rev. D **55**, 3118 (1997), arXiv:hep-ph/9611431.

[27] K. Hagiwara, R. D. Peccei, D. Zeppenfeld, and K. Hikasa, Probing the Weak Boson Sector in e+ e- —> W+ W-, Nucl. Phys. B **282**, 253 (1987).

[28] F. Iachello and D. Kusnezov, Radiative decays of (Q anti-Q) mesons, Phys. Rev. D **45**, 4156 (1992).

[29] S. Godfrey and N. Isgur, Mesons in a Relativized Quark Model with Chromodynamics, Phys. Rev. D **32**, 189 (1985).

[30] D. García Gudiño and G. Toledo Sánchez, Determination of the magnetic dipole moment of the rho meson using four-pion electroproduction data, Int. J. Mod. Phys. A **30**, 1550114 (2015).

[31] H. H. Patel, Package-X: A Mathematica package for the analytic calculation of one-loop integrals, Comput. Phys. Commun. **197**, 276 (2015), arXiv:1503.01469 [hep-ph].

[32] A. Denner, S. Dittmaier, and L. Hofer, Collier: a fortran-based Complex One-Loop LIbrary in Extended Regularizations, Comput. Phys. Commun. **212**, 220 (2017), arXiv:1604.06792 [hep-ph].

[33] R. L. Workman *et al.* (Particle Data Group), Review of Particle Physics, PTEP **2022**, 083C01 (2022).

[34] G. Hernández-Tomé, G. L. Castro, and D. Portillo-Sánchez, ΔL=2 hyperon decays induced by Majorana neutrinos and doubly charged scalars, Phys. Rev. D **105**, 113001 (2022), arXiv:2112.02227 [hep-ph].